Sensitivity and Robustness Aspects of Sensorless Rotor Temperature Estimation Technique for Permanent Magnet Synchronous Motor

M. Ganchev[1], C. Kral[1], T. Wolbank[2]

[1]Austrian Institute of Technology, Vienna, Austria, E-mail: martin.ganchev@ait.ac.at
[2]Vienna University of Technology, Vienna, Austria

***Abstract* – The work focuses on tuning issues of a recently presented sensorless rotor temperature estimation technique for Permanent Magnet Synchronous Motors (PMSMs). The method implies an intermittent injection of a voltage pulse in the d-axis of the motor while keeping the load current zero. Thus, the resulting d-current response depends on both the initial value of the d-current itself and the actual magnetization level of the permanent magnets. Since the magnetization of the magnets depends on the temperature, different d-current slopes are associated with given temperature levels of the magnets. The sensitivity of the method depends strongly on the initial d-current and the injected voltage pulse width. Several method operating conditions will be discussed and compared in terms of sensitivity and influence on the motor performance.**

***Index Terms*—magnet temperature, rotor temperature, permanent-magnet synchronous motor, saturation effects, voltage pulse injection**

I. INTRODUCTION

Permanent Magnet Synchronous Motors (PMSM) are generally the preferred type of machine when high power density and high dynamics are required. It is a fact that modern rare-earth magnets, predominantly used in the manufacturing of PMSMs, undergo reversible demagnetization upon temperature increase. The mostly used type of rare-earth magnet in PMSMs is neodymium-iron-bore (NdFeB). Depending on the environmental temperature and the motor operating conditions, the variation of the magnetization of a typical NdFeB magnet can reach up to 20%. On the one hand monitoring the magnet temperature in PMSM is a safety issue, since irreversible demagnetization of the machine can be prevented. On the other hand it can play a significant role in the torque control of PMSM since a decrease of rotor flux linkage due to temperature dependent demagnetization effects will lead directly to a lower electromagnetic torque output in the machine, [1]. Due to rotation, to obtain the temperature of the rotor by direct measurements is a very cumbersome task. The most common techniques include battery powered devices [2]-[10], infrared sensors, [11]-[14], and slip rings, [15],[16]. A big obstacle is to transfer the rotor temperature signals to a stationary data acquisitioning system. Carrying out such measurements is rather expensive and their application is limited to laboratory and experimental setups since specific instrumentation is normally required. Therefore, significant efforts have been performed recently to develop techniques which do not require any temperature sensors to capture the rotor temperature in PMSMs. Such techniques have been already reported in various papers. The most common approach is a thermal model of the machine. Thermal models imply good knowledge of the geometry, cooling system and especially on the material specific parameters. Their usage is rather limited to industrial applications where environmental and operating conditions are to a great extent known. Some examples of thermal models are given in [17]-[23]. An algorithm to estimate the rotor temperature in PMSM by using flux observer is successfully presented in [24]. This method requires an accurate modeling of the nonlinearities of the inverter. The nonlinear relation between current and flux is defined by a look-up-table (LUT). Furthermore a precise acquisitioning of the machine and inverter parameters is required. An active parameter estimation method by using high frequency signal injection is demonstrated in [13] and [14]. This approach is based on changes in the high frequency stator and rotor resistances due to temperature variation and concludes indirectly the temperature level in the permanent magnets. The robustness and accuracy of the method is influenced by the non-ideal behavior of the inverter.

In this context, the paper focuses on newly gained research findings on a novel temperature-sensorless technique for estimation the temperature of the permanent magnets of PMSM. The main idea of the method is to detect changes in the degree of saturation in the d-axis of the machine which is caused by variation in the magnetization level of the permanent magnets. The basic relationships of the method together with its integration in a common field oriented control (FOC) were first reported in [25]. The current work investigates the method sensitivity and robustness. An interrelationship between the method tuning parameters and their influence on the accuracy of estimating a temperature level is given. An accent is put on analyses to find optimal operating conditions for various performance scenarios and application requirements. The presented results are validated on an Interior Permanent Magnet Synchronous Motors (IPMSM) by directly measuring the rotor temperature via specially designed instrumentation.

II. Definition and Implementation of the Proposed Method

Although the definition of the method has been already reported in [25], for the sake of integrity, the analytical formulation is given here again. In a rotating machine the proposed method requires the knowledge of the rotor position, since the position of the d-axis of the machine should be continuously traced. Thus, by applying a voltage pulse in the d-axis of the motor, the d-current i_d response will vary with changes of the magnetization level of the magnets. The saturation level of the machine experiences the highest effect of the permanent magnet magnetization in its d-axis. Furthermore, this setup supposes that the d-current i_d response is not influenced by the back electromotive force. Using a common three-phase two-level bridge inverter, a corresponding switching pattern can generate a voltage pulse in the pure d-axis of the machine when the angle between the stator and rotor reference frames θ_{el} equals one of the 6 basic space vectors angles ($\theta_{el} = 0°, 60°, 120°,\ 180°, 240°, 300°$). In the current investigation, the definition and implementation of the method is derived by considering voltage pulse applied on the machine at $\theta_{el} = 0°$, which means that dq-rotor reference frame is aligned with the $\alpha\beta$-stationary reference frame of the stator, as shown in Fig. 1. As a consequence, the following relationships for the stator voltage and current components are fulfilled upon voltage pulse generation:

$$u_d \approx u_\alpha;\quad u_q \approx u_\beta;\quad i_d \approx i_\alpha;\quad i_q \approx i_\beta \tag{1}$$

Assuming star connection of the motor, the voltage pulse applied on motor terminals has the following components:

$$u_d \approx u_\alpha = \frac{2}{3}V_{dc} \tag{2}$$

$$u_q \approx u_\beta = 0 \tag{3}$$

where V_{dc} is the inverter dc voltage. Thus, the motor voltage equation in the dq-rotor reference frame can be written as follows:

$$\frac{2}{3}V_{dc} = R_s(i_d + ji_q) + j\omega_r\psi_m + \frac{d}{dt}(L_d i_d + jL_q i_q) \tag{4}$$

where R_s is the stator resistance, ψ_m is the flux linkage produced by the permanent magnets, ω_r is the speed of the rotor reference frame with respect to the stator reference frame, and L_d and L_q are the inductances in the d- and q-direction of the machine respectively. Equation (4) is then decomposed in its real and imaginary components:

$$\frac{2}{3}V_{dc} = R_s i_d + \left(\frac{dL_d}{di_d}i_d + L_d\right)\frac{di_d}{dt} \tag{5}$$

$$-\omega_r\psi_m = R_s i_q + \left(\frac{dL_q}{di_q}i_q + L_q\right)\frac{di_q}{dt} \tag{6}$$

Equation (5) and (6) describe the momentary state of the machine when the rotor and stator reference frames are aligned. The proposed method exploits the resulting relationship from (5). By neglecting the stator resistance voltage drop, equation (5) becomes

$$L_d{}'\frac{di_d}{dt} = \frac{2}{3}V_{dc} \tag{7}$$

$$L_d{}' = \frac{dL_d}{di_d}i_d + L_d\,. \tag{8}$$

It is subject to the condition that at the beginning of the voltage pulse the q-current is zero ($i_q = 0$). Thus, the inductance $L_d{}'$ is predominantly affected by the d-current i_d and the d-axis saturation level of the machine, which is in turn influenced by the magnetization level of the permanent magnets. Cross-coupling effects are neglected here. According to (7), by directly measuring the d-current slope di_d/dt, variation of $L_d{}'$ can be detected. Thus, di_d/dt will change upon changes in the magnetization level of the magnets and can be used as indicator for the magnet temperature T_m. Since (8) has a non-linear character, a distinctive relationship between di_d/dt and T_m for a given machine can be established by a LUT. This is identified during a commissioning phase by direct measurements of T_m or by setting reference temperature levels in the rotor (e.g. in an environmental chamber).

In a practical implementation of the method, detecting the d-axis is confined to predicting the moment when the electrical rotor position equals zero, $\theta_{el} = 0°$. A voltage pulse is then applied in phase ***a*** of the machine such that the electrical rotor position gets zero in the middle of the pulse, as shown in Fig. 2.

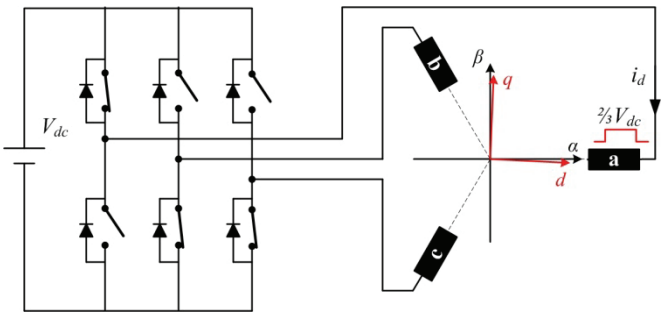

Fig. 1. Voltage pulse injection in the d-axis of the machine at θ_{el}=0°.

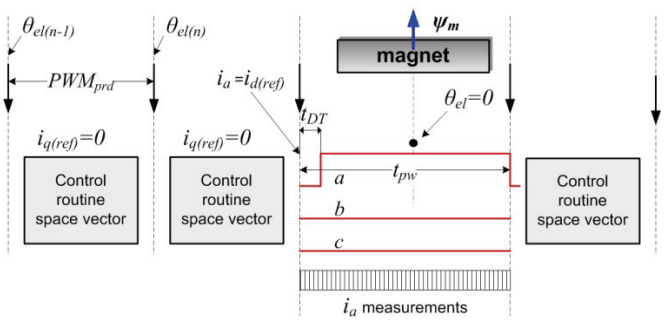

Fig. 2. Time scheduling of the control algorithm and the temperature estimation procedure.

For a given voltage pulse width t_{pw} and inverter pulse width modulation (PWM) period PWM_{prd}, the electrical rotor position θ_{el} is calculated as follows:

$$\theta_{el} = \theta_{el(n)} + \Delta\theta_{el(n)}\left(1 + \frac{t_{pw}}{2PWM_{prd}} + \frac{t_{DT}}{2PWM_{prd}}\right) \quad (9)$$

where

$$\Delta\theta_{el(n)} = \theta_{el(n)} - \theta_{el(n-1)}$$

The last term of (9) accounts for the inverter dead time t_{DT}. It is assumed here that change in the machine speed from one PWM period to the next is negligible ($\Delta\theta_{el(n+1)} = \Delta\theta_{el(n)}$). In a 3-phase symmetrical machine, the d-current i_d is actually the phase current i_a at $\theta_{el} = 0°$. In order to determine the d-current slope, the phase current i_a is oversampled synchronously to the voltage pulse.

III. Method Tuning Parameters

There are two tuning parameters that define an operating point of the method and consequently its sensitivity and robustness: the injected voltage pulse width t_{pw} and the initial d-current reference component $i_{d(ref)}$, which is given by the control circuit.

A. *Voltage Pulse Width*

Generally it is valid that the bigger the voltage pulse width t_{pw}, the more distinctive is the deviation in the d-current response between two different magnet reference temperatures. This is visualized in Fig. 3, where a voltage pulse of 200µs is applied in the machine at standstill and at magnet temperatures of 20°C and 60°C. However, if the voltage pulse width is selected too big with reference to the maximum operating speed, in a rotating machine the electrical relative displacement of the d-axis $\Delta\theta_{el}$ within the voltage pulse duration, as depicted in Fig. 3, will be no longer negligible. In other words, the d-current response will get influenced by the speed. This could be experimentally validated and the results for magnet temperature T_m=20°C are shown in Fig. 5. The displacement of the magnets in radian along a voltage pulse with duration t_{pw} [s] is given by

$$\Delta\theta_{el} = 2\pi p n t_{pw} \quad (10)$$

where p is the number of motor pole pairs and n [rps] is the motor speed. In general, the $\Delta\theta_{el}$ should be kept as small as possible for the following reasons:

- In order to keep valid the assumption made in (1) along the entire voltage pulse duration, especially at higher speeds.
- According to (6), at higher speeds the induced voltage in the q-axis of the machine will produce a rise of the q-current along the voltage pulse. Therefore the voltage pulse should be kept small in order to avoid significant q-current rise that can affect the d-current response di_d/dt due to cross-saturation effects.
- Along the voltage pulse, the α-axis of the motor should see quasi the same permanent magnet flux linkage in a rotating machine as in a machine at standstill.
- A good practice is to keep the resulted d-current response as small as possible for less influence on the motor performance.

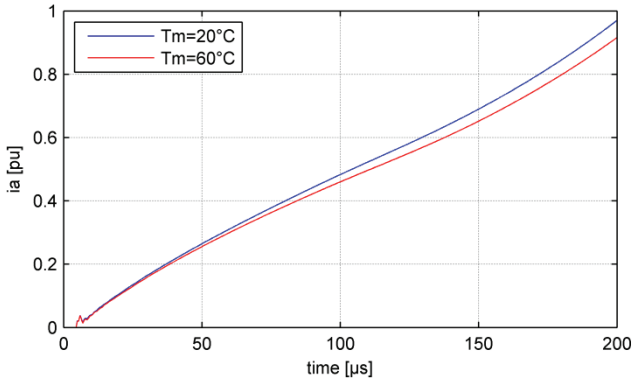

Fig. 3. Current i_a response upon voltage pulse of 200µs in the motor d-axis, with d-current initial value $i_{d(ref)}=0$ at standstill.

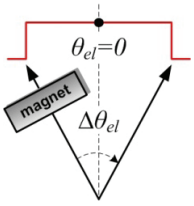

Fig. 4. Relative displacement of the motor d-axis along a voltage pulse.

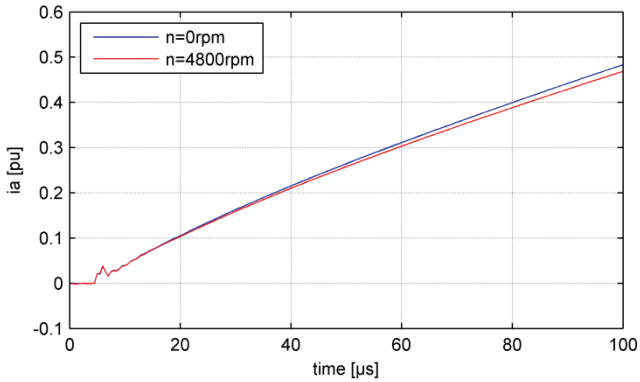

Fig. 5. Current i_a response upon voltage pulse of 100µs in the motor d-axis, with d-current initial value $i_{d(ref)}=0$ at standstill and at nominal speed n=4800rpm (T_m=20°C).

B. *Initial d-current*

Figure Fig. 6 demonstrates a simplified presentation of flux saturation effects that occur in the machine upon voltage pulse injection in the d-axis of the motor while $i_{q(ref)}=0$. By varying the initial d-current $i_{d(ref)}$ different initial saturation levels in the d-axis of the motor can be set before the voltage pulse is generated. An initial d-current $i_{d(ref)}$ for a given pulse width (t_{pw}=constant) provides the most sensitivity when the deviation of the d-current slopes di_d/dt at two different temperatures is the highest. This is the case when the inductance L_d' from (7) starts to decline or in other words, when the stator core starts to saturate in the d-axis along the voltage pulse, as visualized in Fig. 6.

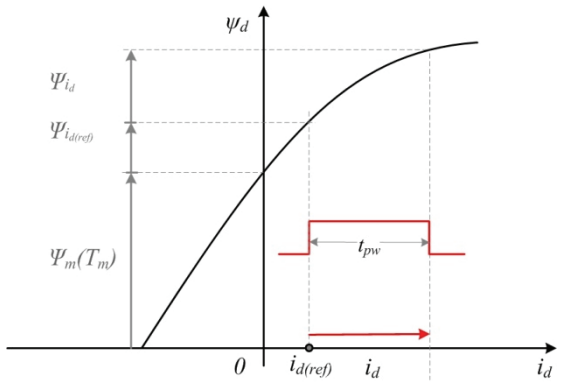

Fig. 6. Simplified presentation of flux saturation effects in the d-axis of the motor due to permanent magnet flux linkage and the d-current excitation ($i_{q(ref)}=0$).

IV. Estimation of Method Sensitivity

A. *Experimental Setup*

The motor under test is an IPMSM with parameters listed in Table I. The rotor is specially manufactured to accommodate thermal sensors. Before the magnets were assembled, holes through the rotor steel with diameter of 2mm were laser drilled in different locations. The used sensors are thermocouples of type K. Fig. 7 shows a rotating instrumentation that measures and converts the thermocouples signals to absolute temperature values and transmits these via infrared optical data link to a stationary receiver. A detailed description of the device is given in [2].

The field oriented space vector control together with the proposed voltage pulse generation is implemented on C6747, a floating point digital signal processor (DSP). The sample rate for the motor currents during the voltage pulse generation is set to 500ns. The inverter operating PWM frequency is set to 20KHz, while the injected voltage pulse width t_{pw} for the magnet temperature estimation can be set arbitrary.

For the validation of a d-current slope di_d/dt when estimating the magnets temperature, the measured phase current i_a curve is linearized by polynomial interpolation

$$y(t) = S_a t + P, \tag{11}$$

where the weighting factor S_a represents the estimated slope of the curve upon voltage pulse generation and the offset P represents $i_{a(t=0)}$, which is assumed to be almost equal the initial d-current $i_{d(ref)}$. Since the voltage pulse is in the range of µs, the unit of the estimated slope S_a is kept here current per unit per µs [pu/µs].

TABLE I: Parameters of the IPMSM Under Test

Nominal power	10 KW
Nominal voltage	440V
Nominal current	25 A
Nominal frequency	320 Hz
Nominal speed	4800 rpm
Magnet type	NdFeB (Vacodym 655 HR)

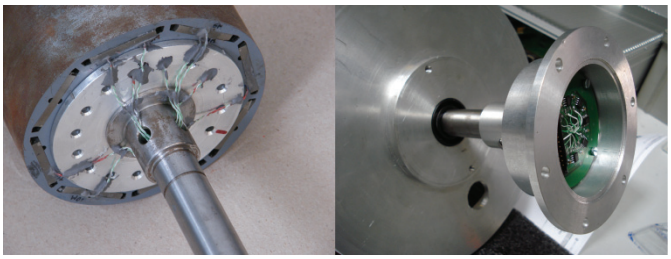

Fig. 7. Realization of contact temperature measurements in the IPMSM under test.

B. *Experimental Results*

The current slopes S_a for two reference temperatures (T_m=20°C and T_m=60°C) are captured at standstill at various method operating points. A method operating point is called here a couple of $i_{d(ref)}$ and t_{pw} values. The deviation of the current slopes between two reference temperatures as a function of the method operating point is depicted in Fig. 8. According to Fig. 8, for $i_{d(ref)}$=0.4pu and t_{pw}=30µs, the deviation of the current slope is the highest which would imply at first sight the highest sensitivity of the method among the investigated operating points.

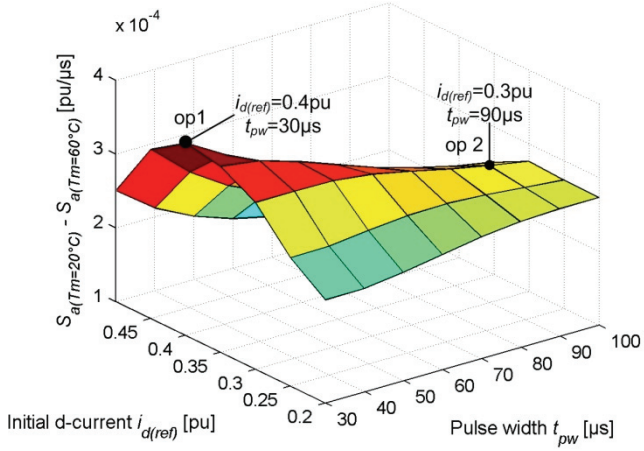

Fig. 8. Current slope deviation upon temperature estimation between two reference magnet temperatures (T_m=20°C and T_m=60°C) as a function of the method operating point.

However, as already mentioned in Section III, the pulse width should be long enough so a distinctive deviation in the corresponding current slopes of two reference temperatures can be generated. This is validated in the following experiment where the influence of the voltage pulse width is investigated in respect to the repetitiveness and the probability to correctly estimate a magnet temperature. For the purpose, measurements are carried out at two operating points with significantly different voltage pulse width: operating point 1 ($i_{d(ref)}$= 0.4pu, t_{pw} = 30µs) and operating point 2 ($i_{d(ref)}$= 0.3pu, t_{pw} = 90µs). As Fig. 8 shows, the selected operating points will characterize with most sensitivity for the respective voltage pulse width. A temperature estimation procedure is conducted in heat-up test at various rotor reference temperatures. Every procedure

consists of 50 measurements. The time interval between two measurements is set to 100ms, thus a whole procedure takes about 7 to 10 seconds to complete. Temperature estimation is conducted at standstill and at motor nominal speed (n=4800rpm). The results from the temperature estimation at operating point 1 are depicted in Fig. 9 and Fig. 10. The slope values in Fig. 9 are the mean values over 50 measurements. For n=4800rpm, the distribution of the 50 measurements for each rotor reference temperature is shown as histogram in Fig. 10. The gray lines in Fig. 10 represent the mean values of S_a. The results from the temperature estimation at operating point 2 are depicted in analogical manner in Fig. 11 and Fig. 12.

C. *Interpretation of the Experimental Results*

As already mentioned in Section III, at higher speeds the voltage pulse width plays a significant role in the accuracy of the proposed temperature estimation method. This is clearly visualized in Fig. 9 and Fig. 11. While at operating point 1 with voltage pulse width of 30µs there is small speed dependency, at operating point 2 with voltage pulse width of 90µs there is a clear offset between the slopes S_a estimated at standstill and at n=4800rpm. If the slopes gained at standstill are considered valid for the entire speed range, the offset will clearly lead to erroneous estimation of the magnet temperature at higher speed. For the machine under test the deviation between temperature estimation at standstill and at nominal speed is less than 6°C for operating point 1 and in the range of -12°C to -15°C for operating point 2. However, at operating point 1, due to the short voltage pulse, the estimated current slopes S_a are not as distinctive as it is the case at operating point 2. This is obvious when comparing the distribution of the measurements in Fig. 10 and Fig. 12. Upon single measurement, the probability to capture the correct temperature of the magnets is lower with shorter voltage pulse than with a bigger one.

From the obtained results, two major strategies for good temperature estimation sensitivity of the method can be concluded. Either a method operating point with short voltage pulse but with higher number of measurements for mean value estimation of the current slope, or a method operating point where a single measurement will give sufficient accuracy but with bigger voltage pulse and obligatory speed compensation.

V. Discussions

In the presented method the stator voltage drop is neglected in (7) so far. If this is considered, the sensitivity of the method can be further slightly increased. However, knowledge of the stator temperature would be required. It is opinion of the authors that due to the short voltage pulse duration no noticeable motor performance degradation is to be expected in a practical application. Currently the presented method can be applied only in applications where the load current can be set to zero for a time duration bigger or at least

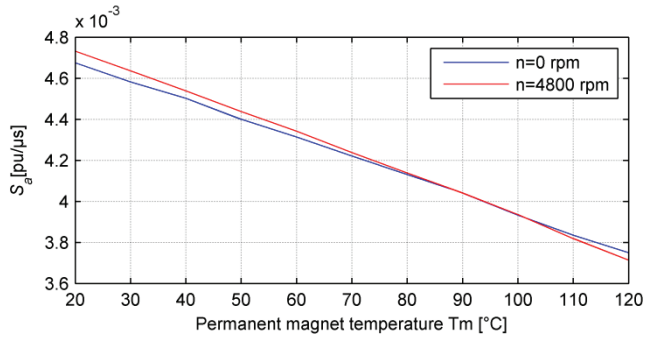

Fig. 9. Mean current slope over 50 measurements at operating point 1 ($i_{d(ref)}=0.4pu$, $t_{pw}=30\mu s$) as a function of the magnet temperature.

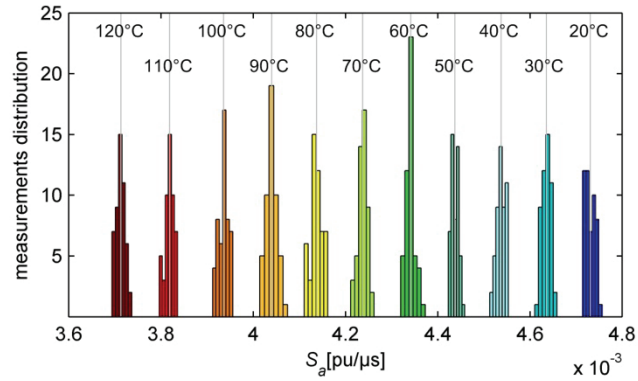

Fig. 10. Distribution of the 50 measurements for each temperature estimation procedure at operating point 1 ($i_{d(ref)}=0.4pu$, $t_{pw}=30\mu s$) and n=4800rpm.

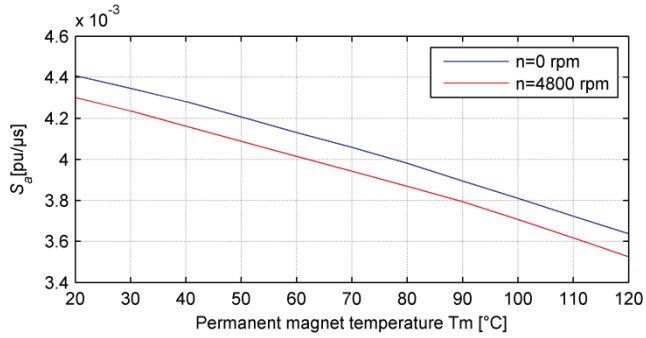

Fig. 11. Mean current slope over 50 measurements at operating point 2 ($i_{d(ref)}=0.3pu$, $t_{pw}=90\mu s$) as a function of the magnet temperature.

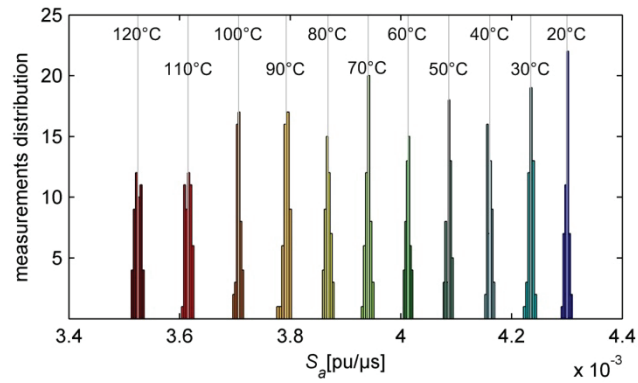

Fig. 12. Distribution of the 50 measurements for each temperature estimation procedure at operating point 2 ($i_{d(ref)}=0.3pu$, $t_{pw}=90\mu s$) and n=4800rpm.

equal 3 to 5 times the electrical motor constant. Subject of ongoing research is to define method applicability under load conditions by investigating the inherent influence of the q-current i_q on the d-current response due to cross-saturation effects.

With respect to a field weakening control, the proposed pulse injection can be implemented by considering negative initial d-current, $i_{d(ref)}<0$. However such investigation is not considered here since the machine under test needs additional d-current excitation ($i_{d(ref)}>0$) to reach a favored saturation level in its d-axis for satisfactory method sensitivity.

VI. CONCLUSION

An estimation of the permanent magnet temperature in an IPMSM has been achieved by detecting the change in the degree of magnetic saturation caused by temperature dependent demagnetization. An extensive investigation of the sensitivity of the method has been presented. It is the opinion of the authors that with the proposed tuning strategies, magnet temperature estimation with very high accuracy can be achieved for the entire motor speed range. The method can be adopted to almost every type of PMSM and easily integrated into a common digital motor control.

REFERENCES

[1] Krishnan, R.; Vijayraghavan, P., "Fast estimation and compensation of rotor flux linkage in permanent magnet synchronous machines," *ISIE '99. Proceedings of the IEEE International Symposium on Industrial Electronics*, vol.2, no., pp.661-666 vol.2, 1999.

[2] M. Ganchev, H. Umschaden, H. Kapeller, "Rotor temperature distribution measuring system," *IECON 2011 - 37th Annual Conference on IEEE Industrial Electronics Society* , vol., no., pp.2006-2011, 7-10 Nov. 2011.

[3] D. J. Tilak Siyambalapitiya, P. G. McLaren, P. P. Acarnley, "A rotor condition monitor for squirrel-cage induction machines," *IEEE Trans. Industry Applications,* vol. IA-23, pp. 334-340, Mar. 1987.

[4] H. Yahoui, G. Grellet, "Measurement of physical signals in rotating part of electrical machine by means of optical fibre transmission," *Instrumentation and Measurement technology Conference 1996, IMTC-96,* vol. 1, pp. 591-596, Jun. 1996.

[5] Hou Zhe, Gu Guobiao, "Wireless rotor temperature measurement system based on MSP430 and nRF401," *International Conference on Electrical Machines and Systems, ICEMS 2008*, pp. 858-861, Oct. 2008.

[6] Xin Xue, V. Sundararajan, W. P. Brithinee, "The application of wireless sensor networks for condition monitoring in three-phase induction motors," *Electrical Insulation Conference and Electrical Manufacturing Expo2007*, pp. 445-448, Oct. 2007.

[7] H. Hafezi, A. Jalilian, "Design and Construction of Induction Motor Thermal Monitoring System," *Universities Power Engineering Conference 2006*, vol. 2, pp. 674-678, Sep. 2006.

[8] Guo Jianzhong, Guo Hui, Hou Zhe, "Rotor temperature monitoring technology of direct-drive permanent magnet wind turbine," *International Conference on Electrical Machines and Systems, ICEMS 2009*, pp. 1-4, Nov. 2009.

[9] Z. Lazarevic, R. Radosavljevic, P. Osmokrovic, "A new thermal observer for squirrel-cage induction motor," *Instrumentation and Measurement technology Conference 1996, IMTC-96,* vol. 1, pp. 610-613, Jun. 1996.

[10] Kovačić, M.; Vražić, M.; Gašparac, I., "Bluetooth wireless communication and 1-wire digital temperature sensors in synchronous machine rotor temperature measurement," *Power Electronics and Motion Control Conference (EPE/PEMC), 2010 14th International* , vol., no., pp.T7-25-T7-28, 6-8 Sept. 2010.

[11] C. Kral, A. Haumer, M. Haigis, H. Lang, H. Kapeller, "Comparison of a CFD analysis and a thermal equivalent circuit model of a TEFC induction machine with measurements," *Energy Conversion, IEEE Transactions on Energy Conversion*, vol.24, no.4, pp.809-818, Dec. 2009.

[12] Stipetic, S.; Kovacic, M.; Hanic, Z.; Vrazic, M., "Measurement of Excitation Winding Temperature on Synchronous Generator in Rotation Using Infrared Thermography," *Industrial Electronics, IEEE Transactions on* , vol.59, no.5, pp.2288-2298, May 2012.

[13] Reigosa, D.D., Briz, F., García, P., Guerrero, J.M., Degner, M.W., "Magnet temperature estimation in surface PM Machines using high-frequency signal injection," *Industry Applications, IEEE Transactions on Industry Applications*, vol.46, no.4, pp.1468-1475, July-Aug. 2010.

[14] Reigosa, D.; Briz, F.; Degner, M.W.; Garcia, P.; Guerrero, J.M.; , "Magnet temperature estimation in surface PM machines during six-step operation," *Energy Conversion Congress and Exposition (ECCE), 2011 IEEE* , vol., no., pp.2429-2436, 17-22 Sept. 2011.

[15] C. Mejuto, M. Mueller, M. Shanel, A. Mebarki, M. Reekie, D. Staton, "Improved synchronous machine thermal modelling," *International Conference on Electrical Machines, ICEM 2008,* pp. 1-6, Sep. 2008.

[16] W. T. Martiny, R. M. McCoy, H. B. Margolis, "Thermal relationships in an induction motor under normal and abnormal operation," *Power Apparatus and System, Part III. Transactions of the American Institute of Electrical Engineers,*, vol. 80, pp. 66-76, Apr. 1961.

[17] E. Odvarka, N. L. Brown, A. Mebarki, M. Shanel, S. Narayanan, and C. Ondrusek, "Thermal modelling of water-cooled axial-flux permanent magnet machine," *5th IET International Conference on Power Electronics, Machines and Drives (PEMD 2010)*, , pp. 1 –5, apr.2010.

[18] Y. Chun, W. Keying, and W. Xiaonian, "Coupled-field thermal analysis of high-speed permanent magnetic generator applied in micro-turbine generator," Proceedings of the Eighth International Conference on Electrical Machines and Systems, ICEMS 2005, vol. 3, pp.2458 – 2461 Vol. 3, sep. 2005.

[19] Boglietti, A.; Cavagnino, A.; Staton, D.; , "Determination of Critical Parameters in Electrical Machine Thermal Models," *IEEE Transactions on Industry Applications*, vol.44, no.4, pp.1150-1159, July-aug. 2008

[20] Boglietti, A.; Cavagnino, A.; Staton, D.; Shanel, M.; Mueller, M.; Mejuto, C.; , "Evolution and Modern Approaches for Thermal Analysis of Electrical Machines," *IEEE Transactions on Industrial Electronics*, vol.56, no.3, pp.871-882, March 2009.

[21] Bauml, T.; Jungreuthmayer, C.; Kral, C.; "An innovative parameterization method for a thermal equivalent circuit model of an interior permanent magnet synchronous machine," *IECON 2011 - 37th Annual Conference on IEEE Industrial Electronics Society* , vol., no., pp.1746-1751, 7-10 Nov. 2011.

[22] Milanfar, P.; Lang, J.H.; , "Monitoring the thermal condition of permanent-magnet synchronous motors," *IEEE Transactions on Aerospace and Electronic Systems*, vol.32, no.4, pp.1421-1429, Oct 1996.

[23] Demetriades, G.D.; de la Parra, H.Z.; Andersson, E.; Olsson, H., "A Real-Time Thermal Model of a Permanent-Magnet Synchronous Motor,", *IEEE Transactions on Power Electronics*, vol.25, no.2, pp.463-474, Feb. 2010.

[24] Specht, A., Böcker, J., "Observer for the rotor temperature of IPMSM," *Power 14th International Electronics and Motion Control Conference (EPE/PEMC), 2010*, vol., no., pp.T4-12-T4-15, 6-8 Sept. 2010.

[25] M. Ganchev, C. Kral, H. Oberguggenberger, T. Wolbank, "Sensorless rotor temperature estimation of permanent magnet synchronous motor," *IECON 2011 - 37th Annual Conference on IEEE Industrial Electronics Society*, vol., no., pp.2018-2023, 7-10 Nov. 2011.